Carbohydrate Polymers 108 (2014) 46–57

Contents lists available at ScienceDirect

Carbohydrate Polymers

journal homepage: www.elsevier.com/locate/carbpol

Novel and diverse fine structures in LiCl–DMSO extracted apple hemicelluloses

Sayani Ray, Jacqueline Vigouroux, Bernard Quémener, Estelle Bonnin, Marc Lahaye*

INRA, UR 1286 Biopolymères – Interactions – Assemblages, rue de la Géraudiere, 44 316 Nantes, France

ARTICLE INFO

Article history:
Received 3 January 2014
Received in revised form 24 February 2014
Accepted 5 March 2014
Available online 25 March 2014

Keywords:
Cell wall
Xyloglucan
Galactoglucomannan
Glucuronoarabinoxylan
LiCl–DMSO
MALDI-TOF MS

ABSTRACT

Hemicelluloses are key polysaccharides in the regulation of the mechanical properties of plant cell walls during organ development and in fruit texture. Their diverse compositions and structures are partially known, in particular with regard to their function in cell walls. To that end, apple hemicelluloses were sequentially extracted by DMSO doped by LiCl followed by potassium hydroxide. The weakly bounded hemicelluloses in the LiCl–DMSO soluble extract were fractionated by ion exchange (AEC) and size exclusion (SEC) chromatographies. The structure of all the extracts and fractions was established by enzymatic fingerprinting using β-glucanase, β-mannanase and β-xylanase. Molecular weight of the fraction was established by HPSEC. MS as well as HPAEC analyses of the enzyme digests revealed the remarkable diversity of apple hemicelluloses. Different xyloglucan (XyG), galactoglucomannan (GgM) and glucuronoarabinoxylan were isolated along the extraction and fractionation process. All LiCl–DMSO soluble fractions were acetyl-esterified. Besides, the LiCl–DMSO soluble XyG differed from the 4 M KOH extracted one essentially on the basis of its molecular weight. At least two populations differing in their content and distribution of glucose and mannose composed GgM. Moreover, galactose ramifications occurred on mannose blocks in the glucose rich fraction. These results open the way for future studies on the complex structure–function relationship of hemicelluloses in plant cell walls.

1. Introduction

Fruit texture is a major quality criterion that influences consumer acceptance and postharvest technical itineraries. It results from coordinated events implying different determinants at several scales involving cell walls (Harker, Redgwell, Hallett, Murray, & Carter, 1997; Waldron, Park, & Smith, 2003). In fleshy fruit, cell walls are assimilated to the primary cell wall of elongating cells due to their composition, hydrophilicity and their viscoelastic mechanical behaviour (Albersheim, Darvill, Roberts, Sederoff, & Staehelin, 2011). The macromolecular assemblies composing them are responsible for the cell shape, provide mechanical support able to sustain large pressures arising from cell turgor and contribute to the structural integrity of the plant organs through cell–cell bonding. These cell walls consist of cellulose microfibrils embedded in and interacting with networks of an amorphous matrix of hemicelluloses, pectins and glycoproteins (Albersheim, Darvill, Roberts, Sederoff, & Staehelin, 2011). On ripening and softening, fleshy fruit cell walls are reorganized and disassembled through the reshuffling and degradation of the matrix polymers that hold cellulose microfibrils in place. The complex biochemical processes involve coordinated sets of "wall-loosening" enzymes and proteins (Brummell, 2006; Goulao & Oliveira, 2008). Wall glycosidases, lyases and esterases modify and/or degrade the complex homogalacturonan and rhamnogalacturonan domains of pectins (Atmodjo, Hao, & Mohnen, 2013) affecting their important role in cell-cell interactions and cell wall rigidity (Jarvis, Briggs, & Knox, 2003; Peaucelle, Braybrook, & Hofte, 2012). Other glycosidases, transglycosylases and expansins act on the fine chemical structure that impacts organization and interactions of the three families of polysaccharides composing the hemicelluloses: xyloglucan (XyG), galactoglucomannan (GgM) and glucurono(arabino)xylan polysaccharides (Scheller & Ulvskov, 2010). Expansins break hydrogen bonds between cellulose and XyG allowing slippage of cellulose microfibrills (Cosgrove, 2005) and making cell wall polysaccharides susceptible to further enzymatic degradation (Brummell

Abbreviations: AIR, alcohol insoluble residue; pDAIR, partially depectinated alcohol insoluble residue; CWR, cell wall residue; HPAEC, high performance anion exchange chromatography; HPSEC, high performance size exclusion chromatography; MALDI-TOF MS, matrix-assisted laser desorption/ionization time of flight mass spectrometry; XyG, xyloglucan; GgM, galactoglucomannan; XyGOs, xyloglucan oligosaccharides; GgMOs, galactoglucomannan oligosaccharides; XOs, xylan oligosaccharides; DMSO, dimethylsulphoxide.

* Corresponding author. Tel.: +33 2 40 67 50 63.
E-mail address: marc.lahaye@nantes.inra.fr (M. Lahaye).

http://dx.doi.org/10.1016/j.carbpol.2014.03.017
0144-8617/

et al., 1999; Wei et al., 2010). Xyloglucan endotransglucosylase/hydrolase (XTH) cleaves and ligates XyG chains to temporarily loosen cell wall (Fry et al., 1992). Other transglycosylases acting on tomato GgM and on papaya xylan have been reported (Johnston et al., 2013; Schröder, Atkinson, & Redgwell, 2009). Glycosidases, some having transglycosylases activities, can also remodel XyG during organ development (Frankova & Fry, 2012; Pauly et al., 2013) with yet unclear functions on wall mechanical properties and fruit texture.

The function of hemicelluloses in plant development and fruit texture has been particularly studied with regard to XyG (Atkinson, Johnston, Yauk, Sharma, & Schröder, 2009; Miedes, Herbers, Sonnewald, & Lorences, 2010; Miedes et al., 2013; Somerville et al., 2004). In apple, an important fruit commodity with contrasted texture affecting consumption and transformation, 11 XTH (Atkinson, Johnston, Yauk, Sharma, & Schröder, 2009) and 8 expansin genes (Trujillo, Mann, & Tong, 2012) have been reported to date targeting potentially XyG and its interactions with cellulose. Differences in gene expression of some of them were shown to contribute to differentiate slowly from rapidly softening apples (Harb, Gapper, Giovannoni, & Watkins, 2012). The number of genes and their regulated expression during development and ripening suggest that they might have different specific functions and targets in the cell wall as the fruit develops and ripens. Besides XyG, little is known on structure, function and enzyme remodelling or metabolizing of apple GgM and heteroxylan.

Apple XyG is a fucogalactoxyloglucan composed of a cellulose-like backbone of 1,4-linked β-D-glucopyranose residues, of which around 75% carry side-chains at *O*-6 (Fry et al., 1993; Voragen, Schols, & Pilnik, 1986). The main side chains are α-D-Xyl*p*-(1→noted) **X** (cf. Fry et al., 1993 for nomenclature), β-D-Gal*p*-(1→2)-α-D-Xyl*p*-(1→noted) **L**, and α-L-Fuc*p*(1→2)-β-D-Gal*p*-(1→2)-α-D-Xyl*p*-(1→noted) **F**. Xyloglucan endoglucanase degrades XyG in a regular manner producing at least one unbranched Glc (**G**) at the reducing end of the oligomers produced (XyGOs). The major apple XyGOs are **XXXG**, **XXFG** and **XLFG** the two latter being present mainly as acetylated derivatives (Galvez-Lopez, Laurens, Quemener, & Lahaye, 2011; Renard, Lomax, & Boon, 1992; Vincken, van den Broek, van der Lei, Beldman, & Voragen, 1997). Acetyl esterification in dicots XyGOs occurs usually on the galactose residue at position *O*-6 and on *O*-3, *O*-4 of the glucan backbone (Kiefer, York, Albersheim, & Darvill, 1990; Pauly, Albersheim, Darvill, & York, 1999).

Alkali-soluble apple GgM were shown to consist of a β-(1→4)-linked Glc*p* and Man*p* backbone, some of which are substituted by single Gal and di-Gal chains at *O-6* position (Nara, Ito, Kato, & Kato, 2004). In the cell wall, GgM are acetylated (Galvez-Lopez, Laurens, Quémener, & Lahaye, 2011). Percy, Melton and Jameson (1997) showed changes in the content of the hemicellulosic mannose (Man) during apple development, indicating fine structural changes in Man containing polymer (GgM). Usually, dicots xylan consists of linear (1,4)-linked-β-D-xylopyranosyl (Xyl) backbones substituted by (1,2)-linked (4-*O*-methyl)-α-D-glucopyranosyl uronic acid and by acetyl esters. Arabinose (Ara) is a minor substituent in dicot hemicelluloses (Scheller & Ulvskov, 2010). In apple, Ara was proposed to be linked on C-2 of xylan (Voragen, Schols, & Pilnik, 1986).

The full knowledge of the mechanisms of enzyme and protein consortia targeting hemicelluloses in the development of fruit texture requires a better understanding of their mode of action and functions in the wall as well as an in depth knowledge of the structural and physicochemical characteristics of their polysaccharide substrates. To that end, the aim of this study focussed on the composition and fine chemical structure of native hemicelluloses isolated from apple. The polysaccharides were extracted by 8.4% LiCl DMSO, as optimized by Assor, Quemener, Vigouroux, and Lahaye (2013), and fractionated by anion exchange and gel permeation chromatography. After they were degraded by glucanase, xylanase and mannanase, the produced oligosaccharides were characterized by high performance anion exchange chromatography and MALDI-TOF mass spectrometry.

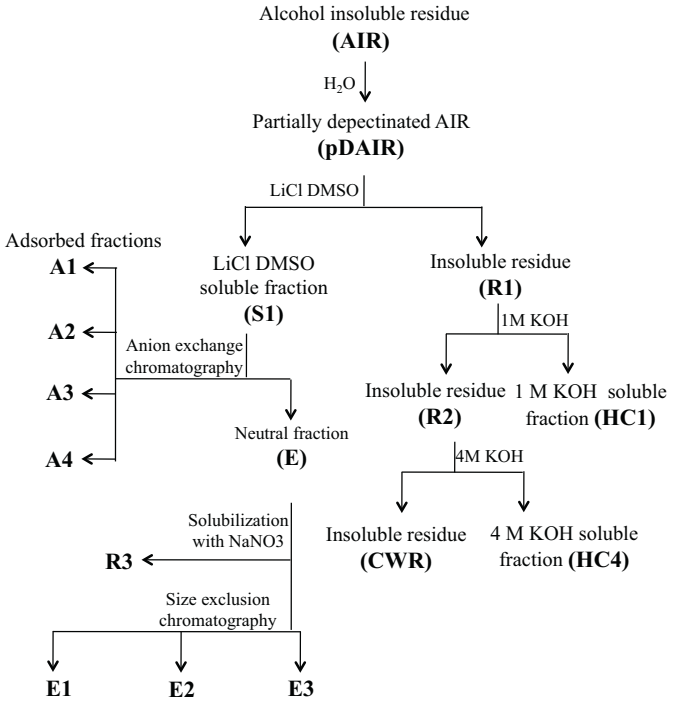

Fig. 1. Sequential extraction and fractionation of hemicelluloses using apple alcohol insoluble residue (**AIR**) as starting material.

2. Material and methods

2.1. Cell wall material preparation

Cell wall material was prepared as an alcohol insoluble residue (**AIR**). Unripe apples (var. Gala; 5.6 kg) were harvested in July 2011 from INRA orchard, Angers, France and kept at 4 °C for 5 months during which the fruits ripened. Apples were peeled, cut and boiled in ethanol 96% (fresh weight/liquid ratio as 1/3 w/v) for 20 min and recovered on a nylon cloth (90 μm). The cell wall material was washed repeatedly with 70% ethanol (solid/liquid ratio as above, 5 times for 4 h) until the ethanol extract was free of sugar (Dubois, Gilles, Hamilton, Rebers, & Smith, 1956). Finally 1.18 kg of humid **AIR** was obtained.

2.2. Isolation of polysaccharides from *AIR*

The sequential extraction procedure used is shown in Fig. 1.

(i) **AIR** (380.9 g fresh weight) was first partially depectinated with water (2 L, 2 h) at 80–85 °C. Solubilized material was separated from the insoluble residue by filtration on a nylon cloth (90 μm) and centrifugation (15 min, 20 °C, 9000 × *g*). The soluble extract (**HWE**) was concentrated, dialyzed against water, concentrated and freeze dried.

(ii) The residue after hot deionized water extraction, named partially depectinated AIR (**pDAIR**), was washed twice with DMSO at 20 °C (1 g of equivalent dry weight for 40 mL of DMSO, 30 min), centrifuged (20 min, 20 °C, 9000 × *g*) and filtered on sintered glass (40–100 μm).

(iii) The DMSO insoluble residue was extracted with 8.4% LiCl–DMSO (1 g equivalent residue dry weight for 200 mL

LiCl–DMSO) at 100 °C during 5 h under continuous agitation and under N_2 (Flores, Stortz, & Cerezo, 2000). The suspension was centrifuged as above and the supernatant solution was filtered on sintered glass (40–100 μm). The insoluble residue (**R1**) was washed twice with LiCl–DMSO and then kept at 4 °C. The LiCl–DMSO extract and washing water were pooled and concentrated by evaporation at 60 °C under vacuum. The concentrated solution was brought to 750 mL with deionised water and precipitated with 4 volumes of 96% ethanol under stirring over night at 4 °C. The crude hemicellulose precipitate (**S1**) was recovered by centrifugation (10 min, 4 °C, 12,600 × *g*) followed by filtration on sintered glass (16–40 μm), washed with ethanol 96% and dried with acetone.

(iv) The insoluble fraction **R1** was extensively washed with deionized water. The remaining hemicelluloses in the residue (1 g residue dry weight) were then extracted with 400 mL of 1 M KOH solution containing 20 mM $NaBH_4$ for 17 h at room temperature (Carpita, 1984). The extract was acidified with cold 4 M acetic acid in an ice bath to pH 6 and dialyzed extensively against deionized water (MWCO 6000–8000). The suspension was centrifuged (20 min, 20 °C, 9000 × *g*) and the supernatant filtered (40–100 μm). **R1** was extracted once more for 1 h in the same conditions. The two extracts were pooled and designated as **HC-1**, and freeze-dried. The residue (**R2**) was submitted to a 4 M KOH extraction following the same protocol. It was washed with 0.1 M acetic acid and with deionised water, freeze-dried and referred to as cell wall residue (**CWR**). The corresponding extracts (**HC-4**) were treated as **HC-1**.

2.3. Fractionation of hemicelluloses

2.3.1. Anion exchange chromatography (AEC)

Crude hemicelluloses fraction **S1** was solubilized in water at a final concentration of 12 g L^{-1}. It was then fractionated on a DEAE-Sepharose Fast Flow column (5 cm × 15 cm, GE Healthcare, Uppsala, Sweden) equilibrated with deionized water. Elution was performed at a flow rate of 2 mL min^{-1} with water (2 column volumes, 600 mL) to recover the unbound fraction (**E**) that was concentrated and freeze-dried. Bound polysaccharides were eluted using a gradient (6 column volumes) from 0 to 100% of NaCl 1 M. Elution was monitored by colorimetric measurement of total sugars (Tollier & Robin, 1979) and uronic acids (Blumenkrantz & Asboe-Hansen, 1973). The fractions eluted in the gradient (**A1**, **A2**, **A3** and **A4**) were concentrated, dialyzed against deionized water, concentrated under vacuum and freeze-dried.

2.3.2. Preparative size-exclusion chromatography (SEC)

Preparative SEC was performed on Sephacryl S-300 column (5 cm × 87 cm, GE Healthcare, Uppsala, Sweden) using 50 mM $NaNO_3$ as eluent at a flow rate 1.6 mL min^{-1}. A solution of **E** was prepared in 50 mM $NaNO_3$ pH 5 at a final concentration of 23.8 g L^{-1} and centrifuged prior to chromatography. The insoluble part was referred to as **R3**. Chromatographic fractions of the $NaNO_3$ soluble **E** were assayed for total neutral sugar and uronic acid contents as above. Fractions **E1**, **E2**, **E3** were pooled according to elution profile, dialysed and freeze dried.

2.4. Chemical cell wall characterization of polysaccharide fractions

2.4.1. Total neutral sugar and uronic acid content

The total neutral sugar content was determined colorimetrically with an automated orcinol/sulphuric acid assay (Tollier & Robin, 1979). Glucose was used as a standard.

Uronic acids content was measured colorimetrically using m-hydroxydiphenyl and concentrated sulphuric acid hydrolysis (Blumenkrantz & Asboe-Hansen, 1973) as automated by Thibault (1979). Galacturonic acid was used as a standard.

2.4.2. Neutral sugar composition

Fractions obtained by sequential extraction were hydrolysed in 1 M H_2SO_4 (2 h, 100 °C) for measurement of individual neutral sugar. Sugars were reduced, acetylated and analyzed as alditol acetate by GLC (Blakeney, Harris, Henry, & Stone, 1983) on a Perkin Elmer AutoSystem (Courtaboeuf, France) mounted with a DB 225 capillary column (J & W Scientific, Folsorn, CA, USA; temperature 205 °C, carrier gas H_2). Standard sugars solution and inositol as internal standard were used for calibration.

2.4.3. Degree of methylation and acetylation

Acetyl ester content was measured by HPLC as the amount of acetic acid released by saponification of 5 mg sample in 1 mL NaOH 0.50 M for 1 h at 4 °C. HPLC was carried out on C18 (4 mm × 250 mm, Lichrospher 100 RP-18e (5 μm), Interchim, France) column thermostated to 25 °C using a refractometric detector (Waters, 2414). An isocratic elution of 4 mM H_2SO_4 was used at a flow rate 1.0 mL min^{-1} (Levigne, Thomas, Ralet, Quemener, & Thibault, 2002). Standard methanol, acetic acid and isopropanol as internal standard were used for calibration.

2.4.4. Protein content

Soluble proteins were measured by the Bradford colorimetric method with the Bio-Rad reagent and using BSA as a standard (Bradford, 1976). Insoluble proteins were measured by the Kjeldahl method (N x 6.25).

2.5. Structural characterization of hemicelluloses

2.5.1. Enzymatic degradations

Cell wall material, chromatographic fractions and extraction residues were degraded by commercial enzymes from Megazyme, Bray, Ireland: endo-1,4-β-glucanase (EGII), endo-1,4-β-xylanase (M2) both from *Trichoderma longibrachiatum*, endo-1,4-β-mannanase from *Aspergillus niger*, α-L-arabinofuranosidase from *Aspergillus niger* and α-D-galactosidase from Guar. The samples (2 mg) were suspended in deionised water containing either 4 U of β-glucanase (Galvez-Lopez, Laurens, Quemener, & Lahaye, 2011), 1.8 U of β-mannanase, 5.2 U of β-xylanase, 10 U of α-L-arabinofuranosidase or 10 U of α-galactosidase and incubated at 40 °C under gentle agitation during 17 h. After centrifugation (15,200 × *g*, 10 min at 20 °C) and enzyme inactivation by 10 min boiling, supernatant solutions were passed through 0.45 μm filter (Millex-Hv, PVDF, Millipore, St Quentin en Yvelines, France) prior to analysis of the oligosaccharides by HPAEC, and MALDI-TOF-MS.

2.5.2. Analysis of oligosaccharides by HPAEC

XyG and GgM oligosaccharides (XyGOs and GgMOs, respectively) were chromatographed through on a Carbo-Pac PA 200 column (3 mm × 250 mm, Dionex, Sunnyvale, USA) whereas xylan oligosaccharides (XOs) were analyzed on a Carbo-Pac PA 1 column (2 mm × 250 mm, Dionex, Sunnyvale, USA) thermostated at 30 °C. Elution was realized using a linear gradient of sodium acetate from 0 to 170 mM in 100 mM NaOH (Quemener, Bertrand, Marty, Causse, & Lahaye, 2007) and detection was done by amperometry using an ED electrochemical detector (Dionex, Sunnyvale, USA).

2.5.3. Analysis of oligosaccharides by MALDI-TOF MS

Enzyme hydrolyzates (1 μL) were mixed with N,N-dimethylaniline/2,5-dihydroxybenzoic acid matrix (1 μL) (Ropartz et al., 2011) on the target plate and left to dry for 3 h at room temperature. For each hydrolyzate, three replicates were realized. MALDI-TOF MS analysis was performed in the positive mode on

Table 1
Yield and chemical composition of apple cell wall fractions on the percent dry weight basis. **HWE,** hot water extract; **pDAIR**, depectinated alcohol insoluble residue; fractions obtained by sequential extraction (cf Fig. 1): LiCl–DMSO (**S1**, **R1**) and KOH (**HC1**, **HC4**, **CWR**); DEAE anion exchange chromatography (**E**, **A1**, **A2**, **A3**, **A4**; cf Fig. 2) and S-300 size exclusion fractionation (**E1**, **E2**, **E3**, **R4**; cf Fig.3). The yields are calculated on a dry weight **pDAIR** basis.

Fraction	Yield	Sugar									Acetyl ester	Methyl ester	Protein
		Rha	Fuc	Ara	Xyl	Man	Gal	Glc	UA	TS			
HWE		1.2	0.0	11.7	1.0	0.6	4.4	2.5	48.9	70.3	0.0	9.4	
pDAIR		1.1	1.5	8.9	7.6	3.5	7.8	24.1	17.4	71.9			
S1	21.1	1.3	2.1	8.9	10.0	7.9	9.3	16.9	27.9	84.3			
R1	61.2	0.9	1.1	6.2	5.7	0.8	5.7	20.9	10.7	52.0			6.7
HC1	6.7	0.8	0.4	3.4	1.5	0.8	3.9	1.3	3.6	15.7			36.3
HC4	9.2	0.4	1.9	2.3	8.1	0.8	4.9	12.9	4.4	35.7			2.2
CWR	35.9	1.1	1.1	6.6	5.8	1.5	5.8	72.9	4.1	98.9			2.1
E	18.3	0.8	2.4	7.8	10.8	9.5	9.2	18.4	5.8	64.7			
A1	0.2	2.3	0.5	3.3	4.4	29.5	19.4	27.8	1.4	88.6	2.5	0.0	1.8
A2	0.2	1.1	0.0	14.9	44.5	1.6	7.9	1.5	11.2	82.7	3.8	0.7	1.8
A3	0.6	4.4	0.2	24.7	13.6	0.0	10.4	0.5	24.3	78.1	2.4	1.3	2.7
A4	1.4	2.0	0.0	3.7	1.4	0.0	2.4	0.4	39.5	49.4	0.6	1.2	2.2
E1	2.9	1.3	4.9	6.8	19.0	1.3	11.1	34.5	12.6	91.5	3.7	0.7	2.7
E2	8.6	0.7	3.8	4.8	14.2	16.0	9.9	34.8	6.8	91.0	4.8	0.4	3.1
E3	0.8	0.6	2.7	5.4	10.6	20.5	9.1	28.9	6.4	84.2	5.8	0.3	2.1
R3	1.4	3.1	0.5	12.0	6.2	3.8	10.9	6.5	24.9	67.9	3.3	1.5	12.7

Sugar composition data are means of duplicates. Rha, rhamnose; Ara, arabinose; Xyl, xylose; Man, mannose; Gal, galactose; Glc, glucose, UA, uronic acid, TS, Total Sugars.

a MALDI-TOF/TOF (Autoflex III Smartbeam, Bruker, Germany) equipped with a Yag laser (355 nm). Analyses were carried out in the reflector mode using a laser frequency of 200 Hz and an accelerating voltage of 19 kV. Spectra were recorded in the mass range m/z 500–3000. A low mass gate value of m/z 500 was selected for analysis in order to avoid saturation of the detector. The instrument was externally calibrated using the monoisotopic masses of main oligosaccharides ($[M+Na]^+$ ion) released from XyG (**XXG**: 791.243 Da, **XXXG**: 1085.338 Da, **XXFGa1**: 1435.459 Da, **XLFGa1**: 1597.512 Da). Nomenclature of XyG oligosaccharides followed that of (Fry et al., 1993) extended to account for acetyl, methyl and uronic acid (UA) groups noted as **a**, **m** and **U**, respectively. Hexoses containing oligosaccharides attributed to GgM were noted **H** and pentoses containing oligosaccharides recovered after xylanase degradation were noted **P**. The figure following the structure codes denoted the number of building structures and acetyl groups in the oligosaccharides ($\mathbf{H_4a_2m_1}$ corresponds to an oligomer with 4 hexoses, 2 acetyl and 1 methyl groups).

2.5.4. Analytical size-exclusion chromatography (HPSEC)

The HPSEC was performed on isolated hemicellulose fractions. The system consisted of a Shodex OHpak SB-G guard column (6 mm × 50 mm, Shodex, Tokyo, Japan) in front of a series of OHpak SB-805HQ and OHpak SB-804HQ columns (8 mm × 300 mm, Shodex, Tokyo, Japan) connected to pump (Jasco PU-1580, Tokyo, Japan) and injector (PerkinElmer, series 200 autosampler, Courtaboeuf, France). Around 3 mg of sample were solubilized in 1 mL of 50 mM $LiNO_3$, centrifuged (10 min, 4 °C, 7400 × g) and filtered through 0.45 μm membrane (Millex-HV, PVDF) prior to injection. Elution was performed with 50 mM $NaNO_3$ at a flow rate of 0.7 mL min^{-1} and monitored by i) differential refractometry (Viscotek VE 3580 RI dectector, Malvern Instruments, Orsay, France), ii) light scattering (LS) detection and iii) differential pressure viscometry (both from Viscotek 270 dual detector, Malvern Instruments, Orsay, France). Weight average molecular weight and molecular weight distribution were obtained using the Omnisec 4.5 software (Software Viscotek 270 dual detector, Malvern Instruments, Orsay,

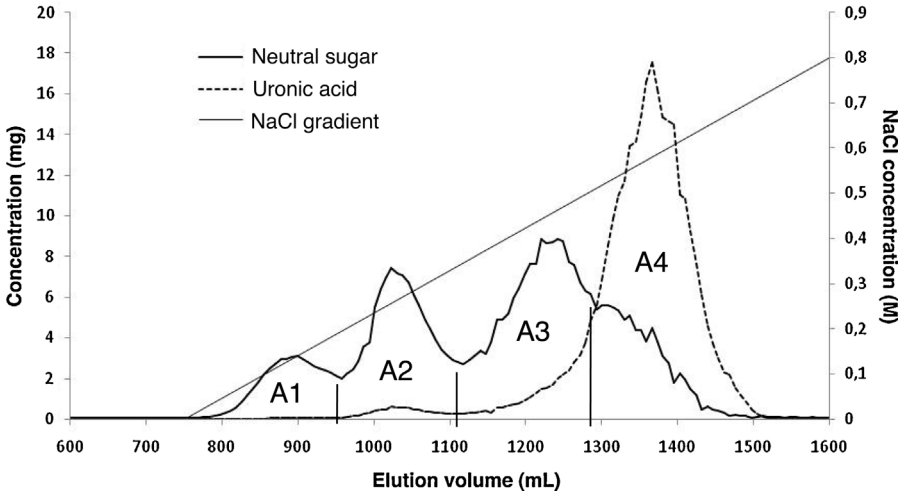

Fig. 2. Fractionation of LiCl–DMSO soluble fraction (**S1**) by anion-exchange chromatography on DEAE-Sepharose FF with a NaCl gradient. The elution was monitored using orcinol and MHDP assays for measuring sugar content.

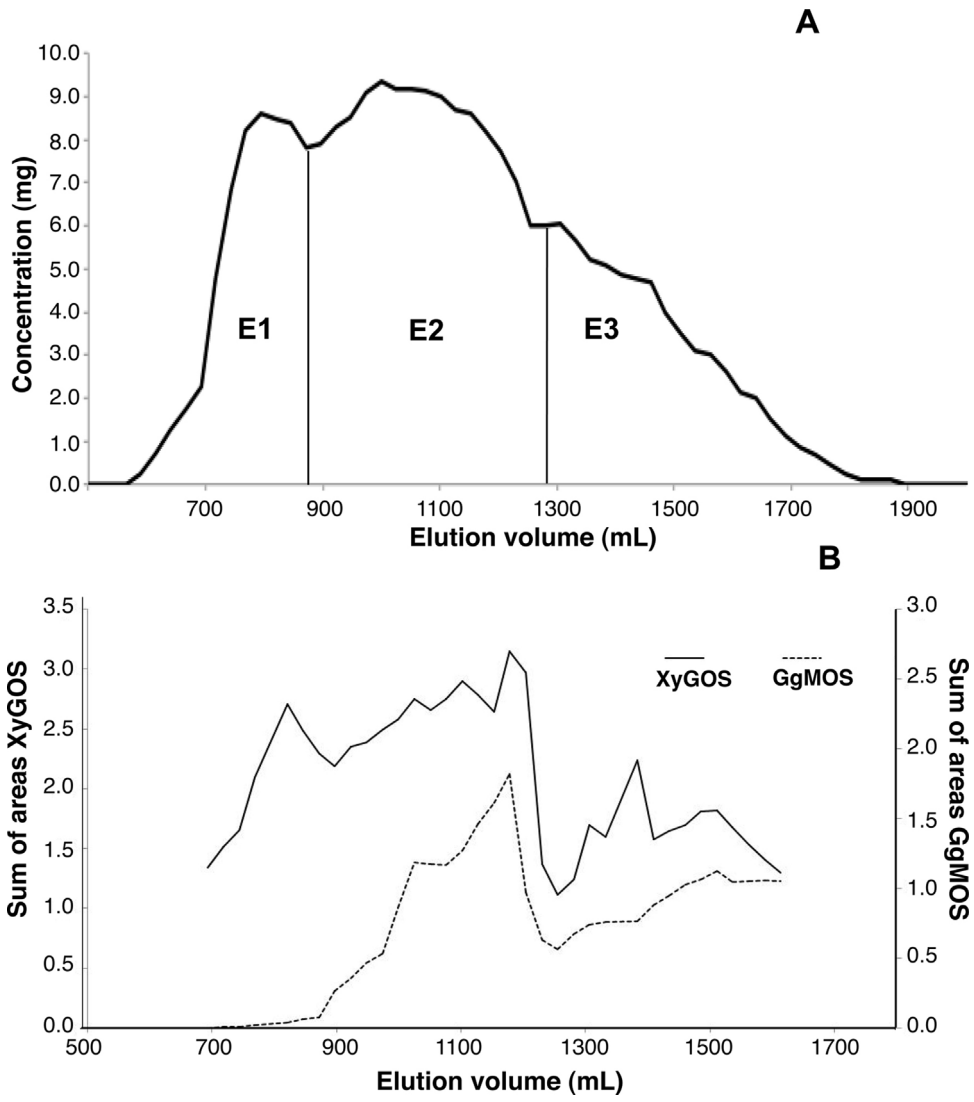

Fig. 3. (A) Size-exclusion chromatography (SEC) on S-300 Sephacryl of the neutral fraction **E** obtained after anion-exchange chromatography. The elution was monitored using orcinol assay for sugar content. (B) The distribution of XyG and GgM through the elution profile of the S-300 was evaluated by considering the specific XyG oligosaccharides (**XXXG**, **XXFG** and **XLFG**; cf Fig. 5) and GgM oligosaccharides released by endo-glucanase degradation of each collected fraction (peaks eluting between 3 and 10 min cf Supplementary Figure 1).

France) and calibration was done with using pullulan-150K (Viscotek, Malvern Instruments, Orsay, France).

3. Results and discussion

3.1. Sequential extraction and fractionation of the cell wall material and their composition

Cell wall material from apple parenchyma was prepared as alcohol insoluble residue (**AIR**). It was then sequentially extracted with hot water, LiCl–DMSO, 1 M and 4 M KOH leaving an insoluble cell wall residue. The overall extraction and fractionation sequences are presented in Fig. 1. The yield and sugar composition of cell wall preparations, soluble and insoluble fractions are given in Table 1. The hot water extract (**HWE**) was mainly composed of uronic acid (UA, 49.2 dry weight% of the extract), arabinose (Ara, 11.7 dw%), galactose (Gal, 4.4 dw%) and contained methyl ester (9.4 dw%) in agreement with the presence of water-soluble pectic polysaccharides (Renard, 2005). The partially depectinated **AIR** (**pDAIR**) was mainly composed of glucose (Glc, 24.1 dw%), UA (17.4 dw%), arabinose (Ara, 8.9 dw%), xylose (Xyl, 7.6 dw%) and mannose (Man, 3.5 dw%) suggesting the presence of cellulosic, hemicellulosic and residual pectic polysaccharides.

Alkali solutions are classically used to extract hemicelluloses since alkali cleaves hydrogen bonds between cellulose and hemicelluloses (Fry, 1988). But at such pH the ester groups are saponified and peeling as well as β-elimination reactions can occur. Other methods have been introduced for extracting hemicelluloses, such as microwave irradiation (Passos, Moreira, Domingues, Evtuguin, & Coimbra, 2014), active oxygen cooking (Shi, Yang, & Lin, 2014), or ionic liquids (Anugwom et al., 2012). Microwave irradiation technique (Passos et al., 2014) was shown to be a very rapid technique to isolate different populations of deacetylated oligomannans according to treatment times. Similarly, cooking for different times and temperatures in oxidative conditions generated by MgO and hydrogen peroxide extracted deacetylated arabinoxylan of different molecular weight (from 3 to 20 kDa). These two extraction methods have limited uses due to the partial degradation of hemicelluloses and particularly their deacetylation. Liquid ionic was used to extract hemicelluloses from spruce wood but the yield and the fine chemical characteristics of the isolated polysaccharides were not reported (Anugwom et al., 2012). According to Hagglund,

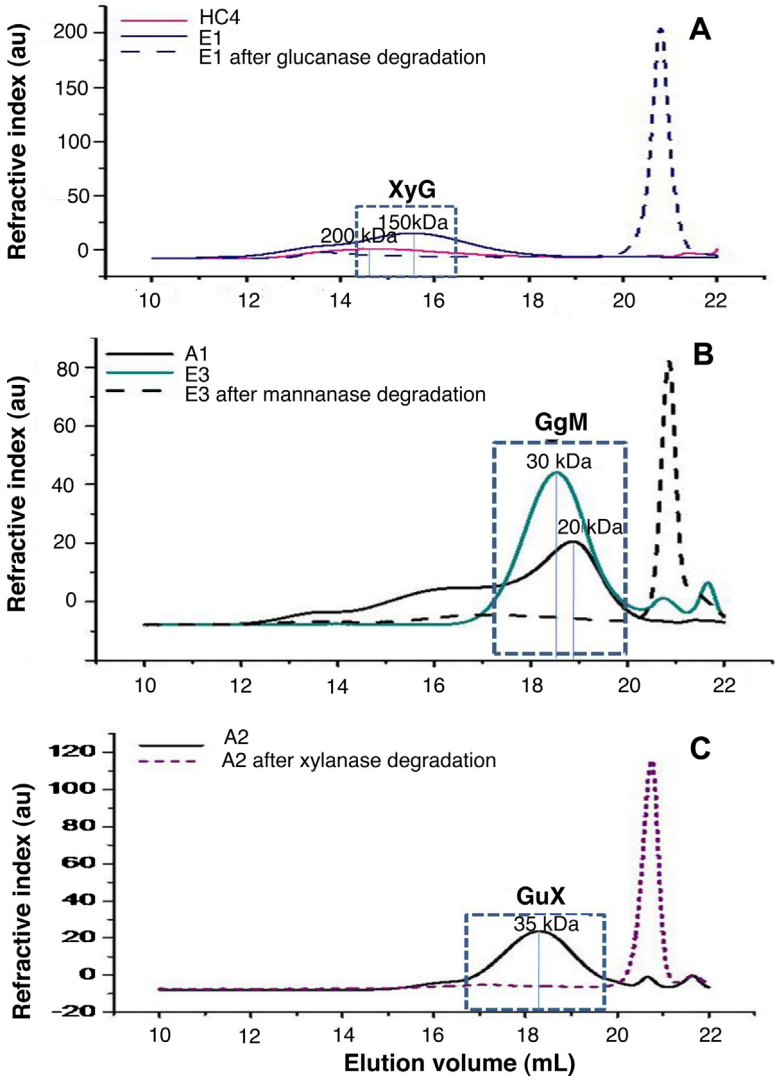

Fig. 4. Normalized high performance size-exclusion chromatogram (HPSEC) of different populations of XyG (A), GgM (B) and glucuronoxylan (C), either as native fraction or after endo-glucanase (A), endo-mannanase (B) and endo-xylanase (C) degradation.

Lindberg, and McPherson (1956) DMSO extracts hemicelluloses in a non-destructive way (Peng, Peng, Xu, & Sun, 2012) where cellulose material exhibits considerable inter-micellar swelling. DMSO has been used in optimized ways with different concentrations of water (Hu, Heitmann, & Rojas, 2008; Willfor, Sundberg, Tenkanen, & Holmbom, 2008) or with 8.4% LiCl (Assor et al., 2013) to extract hemicelluloses. The particular preservation of the acetyl esters on these polysaccharides represents an advantage to characterize their fine structure. In the present work, natively acetylated hemicelluloses were extracted from **pDAIR** with the polar aprotic solvent DMSO doped with 8.4% LiCl according to Assor et al. (2013). This condition successfully extracted acetylated XyG, GgM and glucuronoxylan from tomato cell wall material (Assor et al., 2013). Applied to apple **pDAIR** this extraction yielded 21.1% dry weight (dw%) of soluble polysaccharides (fraction **S1**) that mainly contained 56, 39, 32 and 17% of **pDAIR** Man, UA, Xyl and Glc, respectively, indicating the presence of XyG, GgM and residual pectin or/and glucuronoxylan. On the other hand, **R1** corresponded to 61.2 dw% of **pDAIR** and contained 20.9 dw% Glc attributed to cellulose, and 6.2 dw%, 5.7 dw% and 5.7 dw% of Ara, Xyl and Gal together with 10.7 dw% of UA, indicating the presence of residual pectin and unextracted XyG or/and glucuronoxylan. To access at residual hemicelluloses, **R1** was sequentially treated with 1 M and 4 M KOH. The 1 M KOH soluble fraction (**HC1**, yield 6.7 dw% of **pDAIR**) was composed of Gal, UA and Ara (3.9, 3.6 and 3.4 dw%, respectively) and 36.3 dw% of water-soluble protein indicating the probable presence of arabinogalactan protein. This result contrasted with a previous study (Renard, Lomax, & Boon, 1992) showing that part of apple XyG was extracted with 1 M KOH. Only trace amounts of Xyl and Glc (1.5 and 1.3 dw%, respectively) were measured in **HC1**, showing the absence of XyG in this fraction. In contrast, the 4 M KOH soluble fraction **(HC4**, 9.2 dw% of **pDAIR)** contained mainly Glc, Xyl, Gal and UA (12.9, 8.1, 4.9 and 4.4 dw%, respectively), suggesting the presence of XyG with a trace amount of pectic polysaccharides. Thus, LiCl–DMSO extraction solubilized loosely bound XyG, GgM and pectin whereas part of the tightly bound XyG in the cell wall was solubilized by 4 M KOH. The residue after 4 M KOH extraction (**CWR**) still contained Ara (6.6 dw%), Xyl (5.8 dw%), Gal (5.8 dw%), UA (4.1 dw%), Man (1.5 dw%) attesting for residual pectin and hemicelluloses. The amount of Man in the different fractions showed that about 56% of the initial **pDAIR** Man was recovered from LiCl–DMSO extraction whereas 23% were recovered in **HC1, HC4** and **CWR** and thus were more tightly associated in the wall. Conversely, 21% of Man were lost during the extraction process which was lower than

that reported for tomato (Assor et al., 2013). Overall, about 15 dw% of **pDAIR** were lost with alkaline extractions, attributed to incomplete recovery of polysaccharides and degradation of protein.

Anion exchange chromatography (AEC) allowed the separation of **S1** into one neutral fraction (**E**) and 4 different populations of polysaccharides eluted with the NaCl gradient (**A1**, **A2**, **A3**, **A4**; Fig. 2, Table 1). The neutral fraction **E** contained 62, 69 and 62% of **S1** Xyl, Man, and Glc, respectively, together with 4 dw% of acetyl esters, which were attributed to highly acetyl esterified XyG and GgM. Presence of Ara (7.8 dw%), UA (5.8 dw%), Rha (0.8 dw%) was attributed to a small amount of pectin. Fraction **A1** was slightly bound to the anion exchange matrix as its elution occurred just after the beginning of the NaCl gradient. This neutral fraction was mainly composed of Man, Glc and Gal (39.6, 27.8 and 16.4 dw%, respectively) indicating a population of GgM. The retention of this neutral fraction on the anion exchanger may be related to the characteristics of the Sepharose matrix. This gel is based on cross-linked agarose, which is known to interact through hydrogen bonds with mannans and glucomannans (Dea, 1981). **A2** was essentially made of Xyl, Ara and UA (44.5, 14.9 and 11.2 dw%, respectively), suggesting a substituted xylan. Fraction **A3** was mainly composed of Ara (24.7 dw%), UA (24.3 dw%), Xyl (13.6 dw%), Gal (10.4 dw%) and Rha (4 dw%) indicating the presence of rhamnogalacturonan together with a small amount with glucuronoxylan or xylogalacturonan, a pectic structural domain known to be present in apple pectins (Schols, Bakx, Schipper, & Voragen, 1995). The major fraction from the NaCl gradient **A4** was mainly composed of UA (39.5 dw%), which was attributed to homogalacturonan rich pectin.

Polysaccharides in fraction **E** from the AEC were fractionated on the basis of their hydrodynamic volume through size exclusion chromatography. **E** was dissolved in 50 mM $NaNO_3$ but a part of the fraction remained insoluble (**R3**, 4% of **pDAIR**) likely due to polymer aggregation during the fraction processing. The soluble fraction yielded 3 main peaks, **E1** (3 dw% of **pDAIR**), **E2** (9 dw% of **pDAIR**) and **E3** (1 dw% of **pDAIR**) (Fig. 3A). The sugar analysis (Table 1) suggested **E1** was essentially made of XyG (Glc 34 dw%, Xyl 19 dw% and trace amount of Man), whereas **E2** (Glc 34 dw%, Man 15 dw% and Xyl 14 dw%) and **E3** (Glc 28 dw%, Man 20 dw% and Xyl 10 dw%) were a mixture of XyG and GgM. The distribution of XyG and GgM through the elution profile was evaluated by considering the release of specific oligosaccharides after endo-glucanase degradation of each collected fraction. The result (Fig. 3B) suggested that **E1** contained almost exclusively XyG, whereas **E2** and **E3** contained various proportions of XyG and GgM.

3.2. Fine structural analysis of the hemicellulosic fractions

3.2.1. Xyloglucan

Two different populations almost exclusively composed of XyG (**E1** and **HC4**) were obtained from the **pDAIR** by two approaches. **E1** was obtained after LiCl–DMSO extraction followed by anion exchange and size exclusion chromatographies whereas **HC4** was extracted with 4 M KOH from the LiCl–DMSO residue (Fig. 1). The two fractions differed in their molecular weight: 156 kDa and 200 kDa for **E1** and **HC4**, respectively (Fig. 4A). The disappearance of the major HPSEC peak after treatment of **E1** with endo-β-glucanase confirmed its attribution to XyG (Fig. 4A). As the two fractions behaved differently along the fractionation process, they were believed to be differently associated with the other cell wall polysaccharides due to fine structure differences. These were sought by HPAEC and MALDI-TOF MS analyses of the oligosaccharides released by endo-β-glucanase hydrolysis. The HPAEC elution pattern confirmed the presence of XyGOs (Fig. 5A, B) that were identified using retention times of known oligosaccharides from apple XyG (Renard, Lomax, & Boon, 1992). The two XyGOs profiles were typical of apple XyG with major **XXXG**, **XXFG**, **XLXG** and

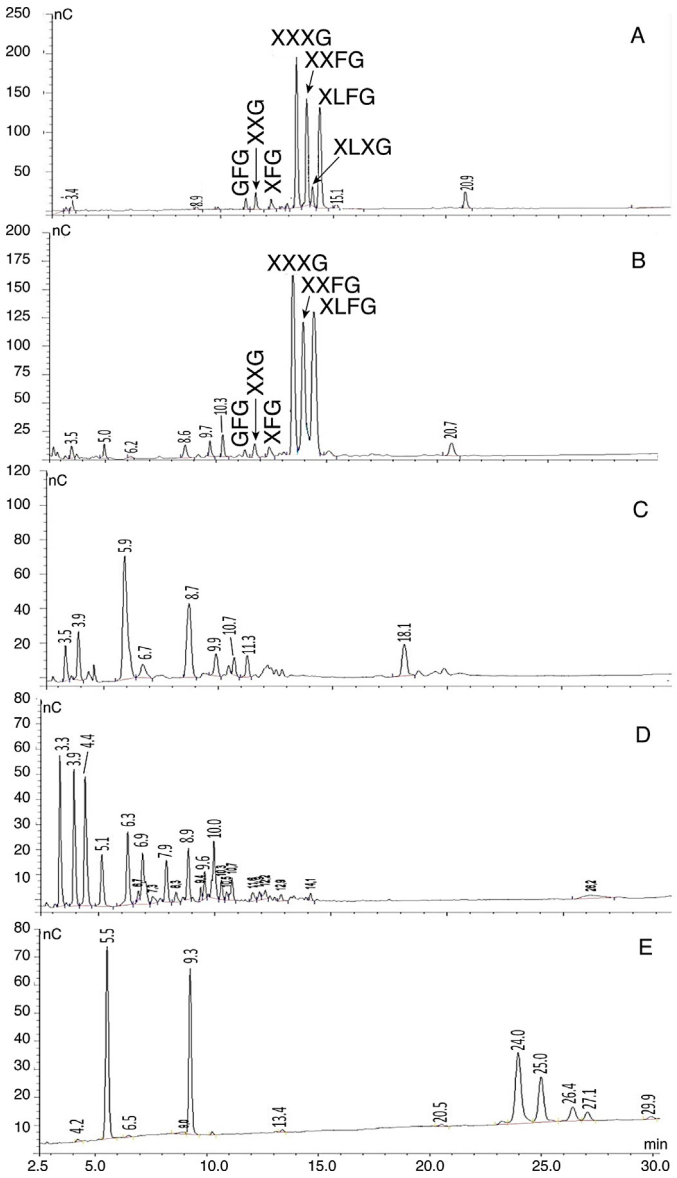

Fig. 5. HPAEC analysis of enzymatic digests of hemicelluloses fraction: endo-glucanase digest of **E1** (A), endo-glucanase digest of **HC4** (B); endo-mannanase digest of **A1** (C), endo-mannanase digest of **E3** (D) and endo-xylanase digest of **A2** (E).

XLFG building blocks together with minor amounts of **XXG**-type oligomers. Beside the loss of acetyl esterification due to the alkaline conditions of **HC4** extraction, the XyGOs profile of the two XyG fractions only differed by the presence of additional small unidentified peaks eluting between 3.3 and 10.3 min on the **HC4** chromatogram. The attribution of the main oligomers was supported by the MALDI-TOF MS spectra of the β-glucanase digest (Fig. 6A, B). Fraction **E1** yielded mainly acetylated XyGOs (Fig. 6A) corresponding to **XLFGa1**, **XXXG** and **XXFGa1** together with minor structures identified as **GFG**, **XFG**, **XXG**, **XLXG**, **XLXGa1**, **XXFG**, **XXFGa2**, **XLFG** and **XLFGa2** as previously reported (Galvez-Lopez, Laurens, Quemener, & Lahaye, 2011; Renard, Lomax, & Boon, 1992; Vincken, van den Broek, van der Lei, Beldman, & Voragen, 1997). The XyGOs MS profile of **HC4** (Fig. 6B) yielded a close profile as that of **E1** taking into account the deacetylation and the potassium adducts of the ions resulting from the KOH extraction of the fraction. This was in agreement with previous work showing no major average structural differences between enzyme and alkali

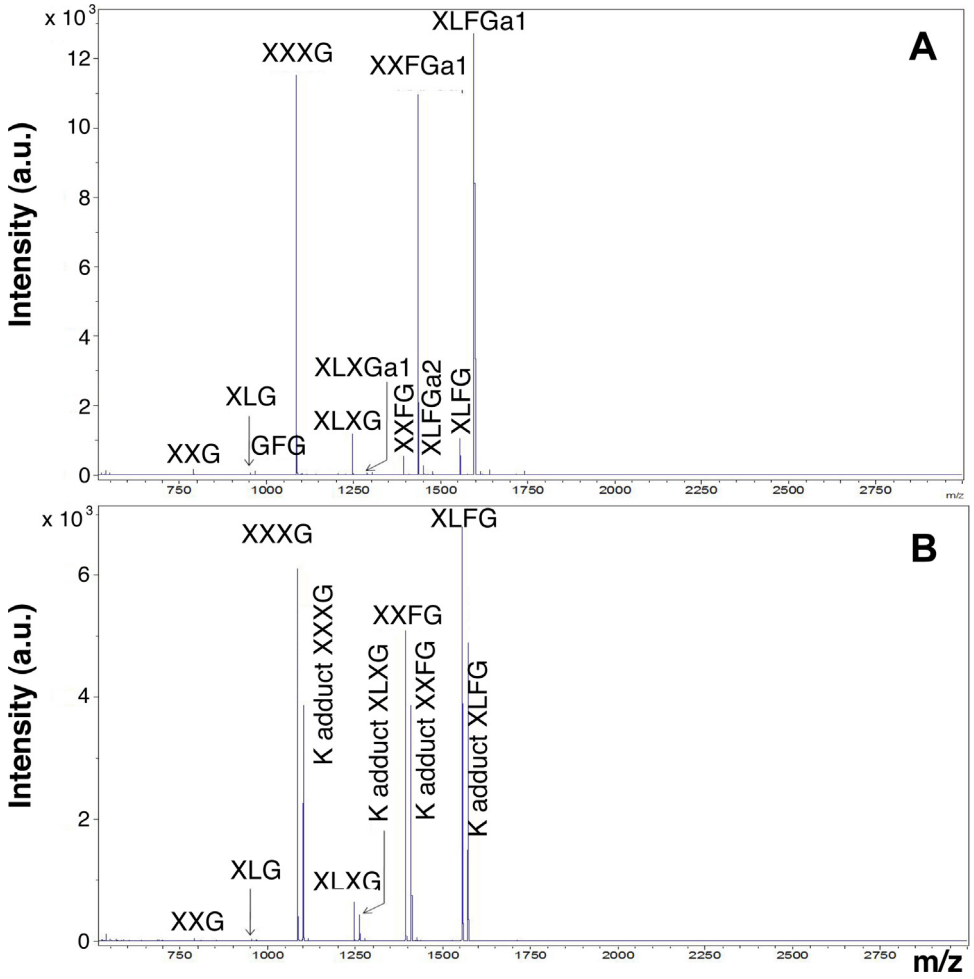

Fig. 6. MALDI-TOF MS spectrum of the endo-glucanase digest of **E1** (A) and **HC4** (B). The nomenclature of oligosaccharides is as described in the text.

extracted XyG from pea (Pauly, Albersheim, Darvill, & York, 1999; Pauly, Qin, Greene, Albersheim, Darvill, & York, 2001). According to the tethered network model of primary cell walls (Albersheim, Darvill, Roberts, Sederoff, & Staehelin, 2011), XyG would act as spacer molecule hydrogen bounded to cellulose and thus prevent cellulose self-aggregation and enable the formation of a strong but flexible XyG-cellulose network. XyG varies in its accessibility to solvents or enzymes (Pauly, Albersheim, Darvill, & York, 1999). Part of it is accessible to endo-glucanase degradation and would include structures tethering cellulose microfibrils in the tethered network model of primary cell walls (Albersheim, Darvill, Roberts, Sederoff, & Staehelin, 2011). A second part involves XyG resisting glucanase degradation and extracted by concentrated alkali. This constitutes the major part of XyG that is thought to coat cellulose microfibrils. A third part, representing a very minor part of XyG (<0.1%), corresponds to domains entrapped within cellulose microfibrils and appears determinant in cell wall mechanical properties (Bootten, Harris, Melton, & Newman, 2004; Park & Cosgrove, 2012; Pauly, Albersheim, Darvill, & York, 1999). Studies reporting mechanical assays after xyloglucanase, cellulase and glucanase degrading the minor cellulose-entrapped XyG, do not support the tethered cell wall model and question the function of XTH in the control of cell wall mechanical properties (Park & Cosgrove, 2012). These authors proposed a model where XyG and cellulose are entangled with a minor amount of XyG interacting with two adjacent cellulose microfibrills. From the present results, apple XyG fractions assumed to have different cell wall affinity in the light of their extraction did not differ on their average fine chemical structure but had different molecular weight. Considering that residual XyG was present in the **CWR**, LiCl–DMSO, 4 M KOH and residual XyG may reflect chains with increasing molecular weight. The longer the chains, the more potential segments interacting with cellulose microfibrils and the lower the diffusion of the entangled and interacting chains will be from the cell wall. One should also consider that enzymatic profiling of XyG yields only a mean view of the fine structure and does not inform on the distribution of the different motifs. Furthermore, the degree of acetylation of more tightly bound XyG could not be measured. In tomato, the acetyl ester content of the cell wall residues after LiCl–DMSO extraction indicated that residual hemicelluloses were still esterified (Assor, Quemener, Vigouroux, & Lahaye, 2013). Block and/or random distribution of **XXXG**- and **XXG**-based motifs as well as acetyl ester substituents may also contribute to the physicochemical properties of XyG in the cell wall. The present scheme of hemicelluloses preparation offers the possibility to have access at different population of XyG that will be useful to study the interaction abilities and mechanical properties of assemblies with cellulose. To the best of our knowledge, it is the first time that acetyl-esterified apple XyG is purified as a single fraction.

3.2.2. *Galactoglucomannan*

Two different populations (**A1** and **E3**) enriched in apple GgM were obtained from the LiCl–DMSO extract. **A1** was the first fraction eluted in the NaCl gradient from the anion exchanger while **E3** was obtained by gel permeation of the fraction unbounded on the anion exchanger (Fig. 1). **A1** and **E3** were first compared with respect to

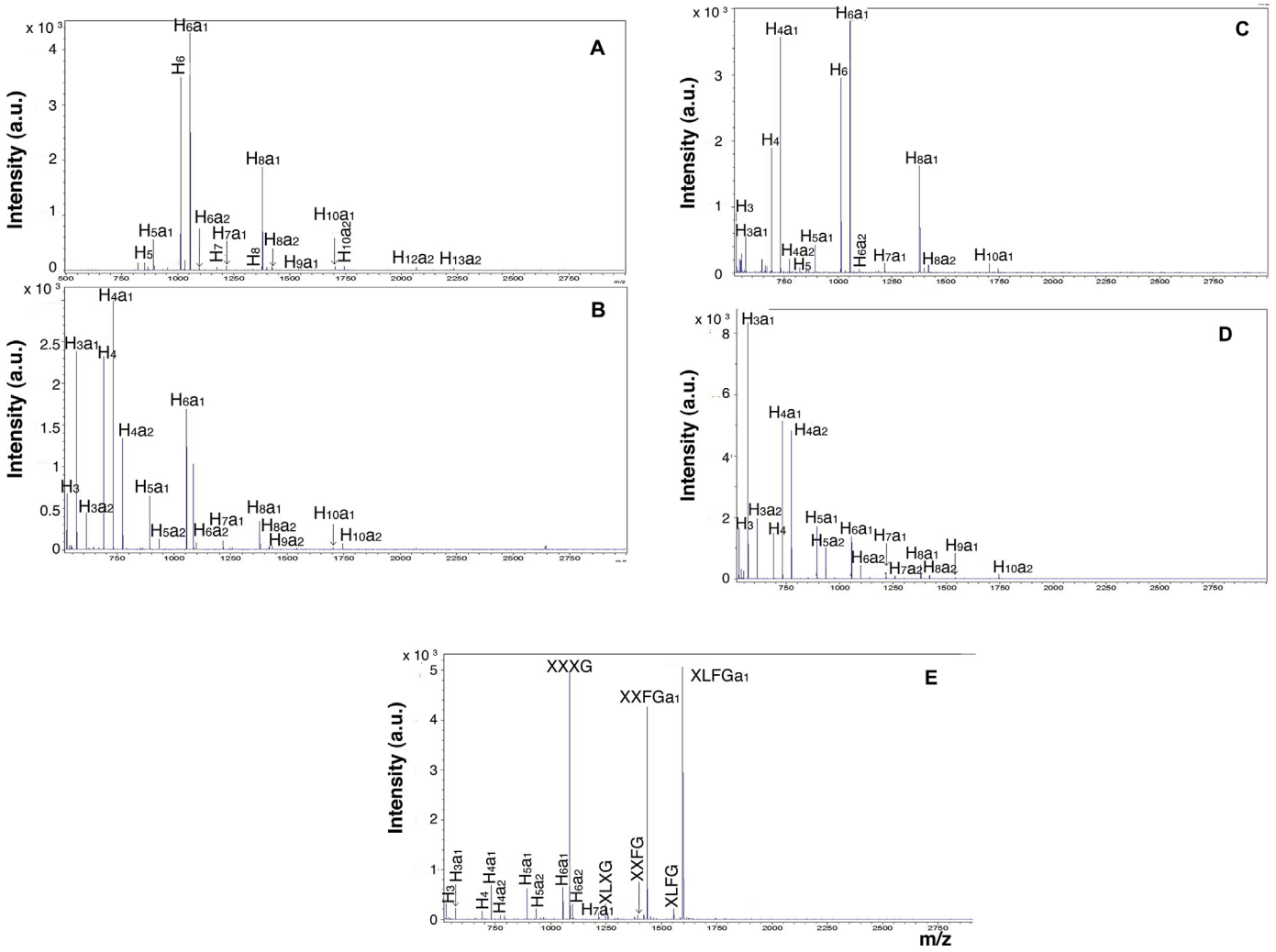

Fig. 7. MALDI-TOF MS spectra of acetylated GgM **A1** (A, B, C) and GgM **E3** (D, E) after degradation by endo-mannanase (A, D), endo-glucanase (B, E) and endo-mannase + α-galactosidase (C). The nomenclature of oligosaccharides is as described in the text.

their molecular weight. **A1** eluted as a single peak at 30 kDa whereas **E3** eluted as a predominant peak at 20 kDa and was contaminated by polysaccharides with higher molecular weight (Fig. 4B). Disappearance of the major **E3** HPSEC peak after endo-β-mannanase treatment confirmed the presence of mannan in this population (Fig. 4B). Differences in their fine structure were assessed by HPAEC and MALDI-TOF MS of oligosaccharides released by β-mannanase hydrolysis. Elution profiles of β-mannanase digests are shown in Fig. 5C, D. The released GgMOs at retention time around 5.9 and 8.7 min were major in **A1** and minor in **E3** whereas peaks eluting up to 5.1 min were major in **E3** and minor or absent in **A1**. The presence of higher molecular weight GgMOs as major structures in **A1** in contrast to **E3** revealed fine structural differences between the two GgM fractions.

The MALDI-TOF spectra of β-mannanase hydrolyzates from **A1** (Fig. 7A) and **E3** (Fig. 7D) demonstrated the presence of a series of more or less acetyl-esterified hexo-oligosaccharides with degrees of polymerization from 3 to 14 attributed to GgM. Mass spectra (Fig. 7A, D) were in agreement with HPAEC chromatograms (Fig. 5C, D): the **A1** mannanase digest contained higher molecular weight oligosaccharides structures compared to **E3**. In **A1** digest, $\mathbf{H_6a_1}$ was the most intense peak followed by $\mathbf{H_6}$ and $\mathbf{H_8a_1}$. **E3** hydrolyzate contained $\mathbf{H_3a_1}$ as highly intense peak followed by $\mathbf{H_4a_1}$, $\mathbf{H_4a_2}$ and others. In order to further investigate the structural differences in these two GgM populations, a sugar composition analysis was realized on the β-mannanase released GgMOs. Results showed a Gal:Man:Glc ratio of 1:1.5:1.4 and 1:4.3:1.4 in **A1** and **E3,** respectively, indicating that **A1** was GgM whereas **E3** was rather a mannan. To confirm this statement **E3** and **A1** were hydrolysed by β-glucanase and the released GgMOs were again compared with that of the mannanase digest. The MALDI-TOF MS of the β-glucanase oligosaccharides from **A1** (Fig. 7B) contained $\mathbf{H_4a_1}$ as major ion followed by $\mathbf{H_3a_1}$, $\mathbf{H_4}$, $\mathbf{H_4a_2}$, and $\mathbf{H_6a_1}$ confirming its GgM nature. In contrast, the **E3** glucanase digest yielded major ions attributed to XyGOs and minor ions attributed to GgMOs (Fig. 7E). The presence of XyG in this fraction agreed with the HPSEC analysis (Fig. 4B), which showed a peak at 15.8 mL of close retention time as the XyG in **E1**. Among the GgMOs, **E3** released minor ions attributed to $\mathbf{H_4a_1}$, $\mathbf{H_5a_1}$ and $\mathbf{H_6a_1}$ followed by $\mathbf{H_3}$, $\mathbf{H_3a_1}$, $\mathbf{H_4}$, $\mathbf{H_4a_2}$, $\mathbf{H_5a_2}$, $\mathbf{H_6a_2}$, and $\mathbf{H_7a_1}$. These minor GgMOs and major XyGOs were also observed by HPAEC (Supplementary Figure 1) indicating that Man in this fraction composed mannan segments. To test for galactose ramifications on the **A1** backbone, this fraction was degraded by a combination of the β-mannanase and a α-galactosidase. The MS profile of the digest obtained (Fig. 7C) was compared with that of GgMOs produced by the β-mannanase alone. The high molecular mass β-mannanase GgMOs ($\mathbf{H_{12}a_2}$ and $\mathbf{H_{13}a_2}$) disappeared after β-mannanase + α-galactosidase treatment with a concomitant appearance of ions attributed to $\mathbf{H_3}$, $\mathbf{H_3a_1}$, $\mathbf{H_4}$, $\mathbf{H_4a_1}$. Thus, Gal ramification was responsible for the presence of high molecular

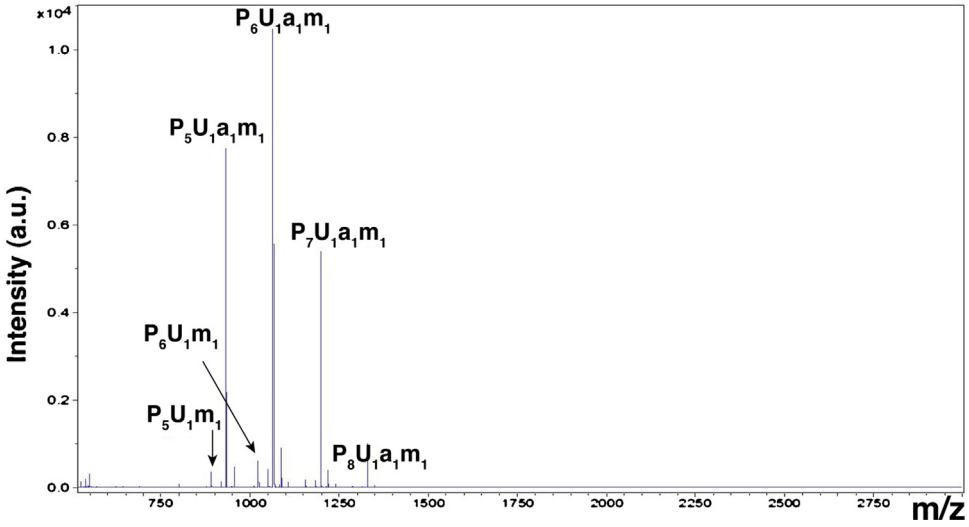

Fig. 8. MALDI-TOF MS spectrum of acetylated glucuronoxylan **A2** after endo-xylanase treatment. Treatment of **A2** by endo-xylanase + α-arabinofuranosidase in combination produced the same profile.

weight oligosaccharides in mannanase released GgMOs from **A1**. Similar treatment of fraction **E3** failed to change the MS GgMOs profile (data not shown). This shows Gal hindered β-mannanase action on **A1** and supports Gal ramification at least on Man. Furthermore, the disappearance of high molecular weight oligosaccharides after galactosidase treatment suggested that galactosylated Man occurred as small blocks in Glc-rich GgM. Nara et al. (2004) suggested Gal ramification is possible on both Glc and Man backbone residues in apple GgM. GgM were reported in other fleshy fruits, such as kiwi and tomato (Prakash et al., 2012; Schröder et al., 2001). In kiwi fruit, Gal ramifications occur on C-6 of mannose and include the disaccharide β-D-Gal-(1→4)-α-D-galactosyl. The function of this hemicellulose is unclear though it is known to be able to hydrogen bound to cellulose (Melton, Smith, Ibrahim, & Schröder, 2009), to be related to cell-cell adhesion in tomato (Ordaz-Ortiz, Marcus, & Knox, 2009), to be likely reshuffled by mannan endotransglycosidase/hydrolase as shown in tomato (Schröder, Wegrzyn, Sharma, & Atkinson, 2006) probably during its metabolism during fruit development (Percy, Melton, & Jameson, 1997). This work revealed that GgM are at least under two different forms in apple cell wall according to the content and distribution of the Man.

3.2.3. Glucuronoxylan

As previously indicated, **A2** was mainly made of Xyl, Ara and UA and also contained high amount of acetyl groups (Table 1), suggesting an acetylated heteroxylan. Its molecular weight was around 35 kDa. Treatment of **A2** by β-xylanase induced the disappearance of the major HPSEC peak (Fig. 4C) and the appearance of a series of oligosaccharides (Fig. 5E), thus confirming its xylan backbone. The MADI-TOF MS analysis of β-xylanase degradation products (Fig. 8) showed the presence of $\mathbf{P_5U_1a_1m_1}$, $\mathbf{P_6U_1a_1m_1}$ and $\mathbf{P_7U_1a_1m_1}$ as major ions and $\mathbf{P_4U_1a_1m_1}$, $\mathbf{P_5U_1m_1}$, $\mathbf{P_6U_1m_1}$ and $\mathbf{P_8U_1a_1m_1}$ as minor ions. The high molecular mass oligomers such as $\mathbf{P_6}$, $\mathbf{P_7}$, $\mathbf{P_8}$ in the end products of **A2** degradation probably originated from different ramifications of the xylan limiting further degradation. In some fleshy fruits like tomato (Assor et al., 2013; Prakash et al., 2012), or tamarillo (do Nascimento et al., 2013) xylans are substituted with (4-*O*-methyl-)glucuronosyl residues resulting in glucuronoxylan. Besides commelinid monocots that usually contain arabinoxylan, arabinosylated glucuronoxylans are rarely reported in the primary cell wall of dicots (Scheller & Ulvskov, 2010). The sugar composition analysis of the xylanase derived oligosaccharides (XOs) from **A2** showed the presence of Ara and Xyl in a ratio of 1:3 (Table 1) indicating the presence of glucuronoarabinoxylan. Ara substitutions on dicot xylans are reported at *O*-2 (Darvill, McNeil, Darvill, & Albersheim, 1980; Zablackis, Huang, Muller, Darvill, & Albersheim, 1995), while 3-linked Ara and doubly substituted Xyl residues have been described in psyllium mucilage and flax seeds, respectively (Fischer, Yu, Gray, Ralph, Anderson, & Marlett, 2004; Naran, Chen, & Carpita, 2008). To investigate the position of Ara as ramification or in the backbone, **A2** fraction was treated with a combination of the xylanase and the α-arabinofuranosidase from *A. niger*. Both the HPAEC elution profiles and MALDI-TOF MS spectra were similar prior and after degradation (data not shown). The arabinofuranosidase used preferentially releases arabinosyl side chains from arabinan and cuts 1–5 linkages better than 1–2 and 1–3 (Kaneko et al., 1998). This result suggested that Ara was not linked in 1–5, but no clear evidence has been found regarding its position in glucuronoxylan. Thus, the presence of a minor amount of xylan in apple hemicelluloses is confirmed (Voragen, Schols, & Pilnik, 1986) most likely as a glucuronoarabinoxylan. Occurring as a distinct fraction from GgM, it did not appear linked to this other hemicellulose as reported under certain conditions in tomato (Prakash et al., 2012).

4. Conclusions

Extraction of hemicelluloses from partially depectinated apple cell walls by LiCl–DMSO revealed that most of these polysaccharides were loosely bounded to the cell wall. The solubility of the acetyl-esterified XyG, GgM, and glucuronoarabinoxylan in LiCl–DMSO and strong base as well as their entanglement in the cellulose rich cell wall residue likely resulted in part from their molecular weight. In addition, at least with regard to XyG, the results question the role of the distribution of the structural motifs and ester substitutions on the interaction and solubility of this polysaccharide. In that respect, acetylated GgM was revealed to exist at least in two forms according to Glc and Man content and distribution. Furthermore, the distribution of galactose ramifications in Glc-rich GgM includes block domains. The diversity and the structural complexity revealed for apple hemicelluloses are at the image of the complex gene families that potentially modify their structure and interaction during fruit development and ripening. The methods set up in this work for obtaining distinct native hemicellulose fractions provide a mean to investigate in more details the cell wall enzymology and the function of these polysaccharides in cell wall mechanical properties and fruit texture.

Acknowledgments

Mass spectrometry analyses were performed within the BIBS platform (INRA Centre Angers-Nantes). SR was supported in part by a scholarship from the Pays de la Loire and Brittany regions within the GlycoOuest research network. The authors thank Roland Robic (IRHS, Angers) for providing the fruits, Marie-Jeanne Crépeau (INRA BIA) and Amani El Akoum (Master student, INRA BIA) for technical contribution.

Appendix A. Supplementary data

Supplementary data associated with this article can be found, in the online version, at http://dx.doi.org/10.1016/j.carbpol.2014.03.017.

References

Albersheim, P., Darvill, A., Roberts, K., Sederoff, R., & Staehelin, A. (2011). *Plant cell walls: From chemistry to biology*. New York: Garland Science, Taylor & Francis Group LLC.

Anugwom, I., Mäki-Arvela, P., Virtanen, P., Willför, S., Sjöholm, R., & Mikkola, J.-P. (2012). Selective extraction of hemicelluloses from spruce using switchable ionic liquids. *Carbohydrate Polymers*, *87*, 2005–2011.

Assor, C., Quemener, B., Vigouroux, J., & Lahaye, M. (2013). Fractionation and structural characterization of LiCl-DMSO soluble hemicelluloses from tomato. *Carbohydrate Polymers*, *94*, 46–55.

Atkinson, R. G., Johnston, S. L., Yauk, Y.-K., Sharma, N. N., & Schröder, R. (2009). Analysis of xyloglucan endotransglucosylase/hydrolase (XTH) gene families in kiwifruit and apple. *Postharvest Biology and Technology*, *51*, 149–157.

Atmodjo, M. A., Hao, Z., & Mohnen, D. (2013). Evolving views of pectin biosynthesis. *Annual Review of Plant Biology*, *64*, 747–779.

Blakeney, A. B., Harris, P. J., Henry, R. J., & Stone, B. A. (1983). A simple and rapid preparation of alditol acetates for monosaccharide analysis. *Carbohydrate Research*, *113*, 291–299.

Blumenkrantz, N., & Asboe-Hansen, G. (1973). New method for quantitative determination of uronic acids. *Analytical Biochemistry*, *54*, 484–489.

Bootten, T. J., Harris, P. J., Melton, L. D., & Newman, R. H. (2004). Solid-state (13)C-NMR spectroscopy shows that the xyloglucans in the primary cell walls of mung bean (*Vigna radiata* L.) occur in different domains: A new model for xyloglucan-cellulose interactions in the cell wall. *Journal of Experimental Botany*, *55*, 571–583.

Bradford, M. M. (1976). A rapid and sensitive method for the quantitation of microgram quantities of protein utilizing the principle of protein-dye binding. *Analytical Biochemistry*, *72*, 248–254.

Brummell, D. A. (2006). Cell wall disassembly in ripening fruit. *Functional Plant Biology*, *33*, 103–119.

Brummell, D. A., Harpster, M. H., Civello, P. M., Palys, J. M., Bennett, A. B., & Dunsmuir, P. (1999). Modification of expansin protein abundance in tomato fruit alters softening and cell wall polymer metabolism during ripening. *Plant Cell*, *11*, 2203–2216.

Carpita, N. (1984). Fractionation of hemicelluloses from maize cell walls with increasing concentrations of alkali. *Phytochemistry*, *23*, 1089–1093.

Cosgrove, D. J. (2005). Growth of the plant cell wall. *Nature Reviews Molecular Cell Biology*, *6*, 850–861.

Darvill, J. E., McNeil, M., Darvill, A. G., & Albersheim, P. (1980). Structure of plant cell walls. XI. Glucuronoarabinoxylan, a second hemicellulose in the primary cell walls of suspension-cultured sycamore cells. *Plant Physiology*, *66*, 1135–1139.

Dea, I. C. M. (1981). Specificity of interactions between polysaccharide helices and β-1,4-linked polysaccharides. *Proceedings of the American Chemical Society Conferences*, *150*, 439–453.

do Nascimento, G. E., Hamm, L. A., Baggio, C. H., Werner, M. F. d. P., Iacomini, M., & Cordeiro, L. M. C. (2013). Structure of a galactoarabinoglucuronoxylan from tamarillo (*Solanum betaceum*), a tropical exotic fruit, and its biological activity. *Food Chemistry*, *141*, 510–516.

Fischer, M. H., Yu, N. X., Gray, G. R., Ralph, J., Anderson, L., & Marlett, J. A. (2004). The gel-forming polysaccharide of psyllium husk (*Plantago ovata* Forsk). *Carbohydrate Research*, *339*, 2009–2017.

Flores, M. L., Stortz, C. A., & Cerezo, A. S. (2000). Studies on the skeletal cell wall of the cystocarpic stage of the red seaweed Iridaea undulosa B. Part II. Fractionation of the cell wall and methylation analysis of the inner core-fibrillar polysaccharides. *International Journal of Biological Macromolecules*, *27*, 21–27.

Frankova, L., & Fry, S. C. (2012). Trans-alpha-xylosidase and trans-β-galactosidase activities, widespread in plants, modify and stabilize xyloglucan structures. *Plant Journal*, *71*, 45–60.

Fry, S. C. (1988). *The growing plant cell wall: Chemical and metabolic analysis*. New York: Longman Scientific and Technical.

Fry, S. C., Smith, R. C., Renwick, K. F., Martin, D. J., Hodge, S. K., & Matthews, K. J. (1992). Xyloglucan endotransglycosylase, a new wall-loosening enzyme activity from plants. *Biochemical Journal*, *282*, 821–828.

Fry, S. C., York, W. S., Albersheim, P., Darvill, A., Hayashi, T., Joseleau, J. P., et al. (1993). An unambiguous nomenclature for xyloglucan-derived oligosaccharides. *Physiologia Plantarum*, *89*, 1–3.

Galvez-Lopez, D., Laurens, F., Quemener, B., & Lahaye, M. (2011). Variability of cell wall polysaccharides composition and hemicellulose enzymatic profile in an apple progeny. *International Journal of Biological Macromolecules*, *49*, 1104–1109.

Goulao, L. F., & Oliveira, C. M. (2008). Cell wall modifications during fruit ripening: When a fruit is not the fruit. *Trends in Food Science and Technology*, *19*, 4–25.

Hagglund, E., Lindberg, B., & McPherson, J. (1956). Dimethylsulphoxide, a solvent for hemicelluloses. *Acta Chemica Scandinavica*, *10*, 1160–1164.

Harb, J., Gapper, N. E., Giovannoni, J. J., & Watkins, C. B. (2012). Molecular analysis of softening and ethylene synthesis and signaling pathways in a non-softening apple cultivar, 'Honeycrisp' and a rapidly softening cultivar, 'McIntosh'. *Postharvest Biology and Technology*, *64*, 94–103.

Harker, F. R., Redgwell, R. J., Hallett, I. C., Murray, S. H., & Carter, G. (1997). Texture of fresh fruit. *Horticultural Reviews*, *20*, 121–224.

Hu, G., Heitmann, J., & Rojas, O. (2008). Feedstock pretreatment strategies for producing ethanol from wood, bark, and forest residues. *BioResources*, *3*, 270–294.

Jarvis, M. C., Briggs, S. P. H., & Knox, J. P. (2003). Intercellular adhesion and cell separation in plants. *Plant Cell Environment*, *26*, 977–989.

Johnston, S. L., Prakash, R., Chen, N. J., Kumagai, M. H., Turano, H. M., Cooney, J. M., et al. (2013). An enzyme activity capable of endotransglycosylation of heteroxylan polysaccharides is present in plant primary cell walls. *Planta*, *237*, 173–187.

Kaneko, S., Arimoto, M., Ohba, M., Kobayashi, H., Ishii, T., & Kusakabe, I. (1998). Purification and substrate specificities of two α-L-arabinofuranosidases from Aspergillus awamori IFO 4033. *Applied and Environmental Microbiology*, *64*, 4021–4027.

Kiefer, L. L., York, W. S., Albersheim, P., & Darvill, A. G. (1990). Structural characterization of an arabinose-containing heptadecasaccharide enzymatically isolated from sycamore extracellular xyloglucan. *Carbohydrate Research*, *197*, 139–158.

Levigne, S., Thomas, M., Ralet, M.-C., Quemener, B., & Thibault, J. F. (2002). Determination of the degrees of methylation and acetylation of pectins using a C18 column and internal standards. *Food Hydrocolloids*, *16*, 547–550.

Melton, L. D., Smith, B. G., Ibrahim, R., & Schröder, R. (2009). Mannans in primary and secondary plant cell walls. *New Zealand J. Forestry Sci.*, *39*, 153–160.

Miedes, E., Herbers, K., Sonnewald, U., & Lorences, E. P. (2010). Overexpression of a cell wall enzyme reduces xyloglucan depolymerization and softening of transgenic tomato fruits. *Journal of Agricultural and Food Chemistry*, *58*, 5708–5713.

Miedes, E., Suslov, D., Vandenbussche, F., Kenobi, K., Ivakov, A., Van Der Straeten, D., et al. (2013). Xyloglucan endotransglucosylase/hydrolase (XTH) overexpression affects growth and cell wall mechanics in etiolated *Arabidopsis* hypocotyls. *Journal of Experimental Botany*, *64*, 2481–2497.

Nara, K., Ito, S., Kato, K., & Kato, Y. (2004). Isolation of galactoglucomannan from apple hemicellulosic polysaccharides with binding capacity to cellulose. *Journal of Applied Glycoscience*, *51*, 321–325.

Naran, R., Chen, G., & Carpita, N. C. (2008). Novel rhamnogalacturonan I and arabinoxylan polysaccharides of flax seed mucilage. *Plant Physiology*, *148*, 132–141.

Ordaz-Ortiz, J. J., Marcus, S. E., & Knox, J. P. (2009). Cell wall microstructure analysis implicates hemicellulose polysaccharides in cell adhesion in tomato fruit pericarp parenchyma. *Molecular Plant*, *2*, 910–921.

Park, Y. B., & Cosgrove, D. J. (2012). A revised architecture of primary cell walls based on biomechanical changes induced by substrate-specific endoglucanases. *Plant Physiology*, *158*, 1933–1943.

Passos, C. P., Moreira, A. S. P., Domingues, M. R. M., Evtuguin, D. V., & Coimbra, M. A. (2014). Sequential microwave superheated water extraction of mannans from spent coffee grounds. *Carbohydrate Polymers*, *103*, 333–338.

Pauly, M., Albersheim, P., Darvill, A., & York, W. S. (1999). Molecular domains of the cellulose/xyloglucan network in the cell walls of higher plants. *Plant Journal*, *20*, 629–639.

Pauly, M., Gille, S., Liu, L., Mansoori, N., de Douza, A., Schultink, A., et al. (2013). Hemicellulose biosynthesis. *Planta*, *238*, 627–642.

Pauly, M., Qin, Q., Greene, H., Albersheim, P., Darvill, A., & York, W. S. (2001). Changes in the structure of xyloglucan during cell elongation. *Planta*, *212*, 842–850.

Peaucelle, A., Braybrook, S., & Hofte, H. (2012). Cell wall mechanics and growth control in plants: The role of pectins revisited. *Frontiers in Plant Science*, *3* http://dx.doi.org/10.3389/fpls.2012.00121

Peng, F., Peng, P., Xu, F., & Sun, R. C. (2012). Fractional purification and bioconversion of hemicelluloses. *Biotechnology Advances*, *30*, 879–903.

Percy, A. E., Melton, L. D., & Jameson, P. E. (1997). Xyloglucan and hemicelluloses in the cell wall during apple fruit development and ripening. *Plant Science*, *125*, 31–39.

Prakash, R., Johnston, S. L., Boldingh, H. L., Redgwell, R. J., Atkinson, R. G., Melton, L. D., et al. (2012). Mannans in tomato fruit are not depolymerized during ripening despite the presence of endo-β-mannanase. *Journal of Plant Physiology*, *169*, 1125–1133.

Quémener, B., Bertrand, D., Marty, M., Causse, M., & Lahaye, M. (2007). Fast data preprocessing for chromatographic fingerprints of tomato cell wall polysaccharides using chemometric methods. *Journal of Chromatography A*, *1141*, 41–49.

Renard, C. M. G. C. (2005). Variability in cell wall preparations: Quantification and comparison of common methods. *Carbohydrate Polymers*, *60*, 515–522.

Renard, C. M. G. C., Lomax, J. A., & Boon, J. J. (1992). Apple-fruit xyloglucan: A comparative study of enzyme digests of whole cell walls and of alkali-extracted xyloglucans. *Carbohydrate Research*, *232*, 303–320.

Ropartz, D., Bodet, P. E., Przybylski, C., Gonnet, F., Daniel, R., Fer, M., et al. (2011). Performance evaluation on a wide set of matrix-assisted laser desorption ionization matrices for the detection of oligosaccharides in a high-throughput mass

spectrometric screening of carbohydrate depolymerizing enzymes. *Rapid Communication in Mass Spectrometry*, *25*, 2059–2070.
Scheller, H. V., & Ulvskov, P. (2010). Hemicelluloses. *Annual Review in Plant Biology*, *61*, 263–289.
Schols, H. A., Bakx, E. J., Schipper, D., & Voragen, A. G. J. (1995). A xylogalacturonan subunit present in the modified hairy regions of apple pectin. *Carbohydrate Research*, *279*, 265–279.
Schröder, R., Atkinson, R. G., & Redgwell, R. (2009). Re-interpreting the role of endo-β-mannanases as mannan endotransglycosylase/hydrolases in the plant cell wall. *Annals of Botany*, *104*, 197–204.
Schröder, R., Nicolas, P., Vincent, S. J. F., Fischer, M., Reymond, S., & Redgwell, R. J. (2001). Purification and characterisation of a galactoglucomannan from kiwifruit (*Actinidia deliciosa*). *Carbohydrate Research*, *331*, 291–306.
Schröder, R., Wegrzyn, T. F., Sharma, M. N., & Atkinson, R. G. (2006). LeMAN4 endo-β-mannanase from ripe tomato fruit can act as a mannan transglycosylase or hydrolase. *Planta*, *224*, 1091–1102.
Shi, J., Yang, Q., & Lin, L. (2014). The structural features of hemicelluloses dissolved out at different cooking stages of active oxygen cooking process. *Carbohydrate Polymers*, *104*, 182–190.
Somerville, C., Bauer, S., Brininstool, G., Facette, M., Hamann, T., Milne, J., et al. (2004). Toward a system approach to understanding plant cell walls. *Science*, *306*, 2206–2211.
Thibault, J. F. (1979). Automatisation du dosage des substances pectiques par la méthode au meta-hydroxydiphenyl. *Lebensmittel-Wissenschaft & Technologie*, *12*, 247–251.
Tollier, M. T., & Robin, J. P. (1979). Adapation de la méthode à l'orcinol-sulfurique au dosage automatique des glucides neutres totaux: Conditions d'application aux extraits d'origine végétale. *Annals des Technologies agricoles*, *28*, 1–15.
Trujillo, D. I., Mann, H. S., & Tong, C. B. S. (2012). Examination of expansin genes as related to apple fruit crispness. *Tree Genetics & Genomes*, *8*, 27–38.
Vincken, J.-P., van den Broek, L. A. M., van der Lei, D. D., Beldman, G., & Voragen, A. G. J. (1997). Fungal and plant xyloglucanases may act in concert during liquefaction of apples. *Journal of the Science of Food and Agriculture*, *73*, 407–416.
Voragen, A. G. J., Schols, H. A., & Pilnik, W. (1986). Structural features of the hemicellulose polymers or apples. *Zeitung Lebensmittel Unters Forschung*, *183*, 105–110.
Waldron, K. W., Park, M. L., & Smith, A. C. (2003). Plant cell walls and food quality. *Comprehensive Reviews in Food Science and Food Safety*, *2*, 101–119.
Wei, W., Yang, C., Luo, J., Lu, C. M., Wu, Y. J., & Yuan, S. (2010). Synergism between cucumber alpha-expansin, fungal endoglucanase and pectin lyase. *Journal of Plant Physiology*, *167*, 1204–1210.
Willfor, S., Sundberg, K., Tenkanen, M., & Holmbom, B. (2008). Spruce-derived mannans — a potential raw material for hydrocolloids and novel advanced natural materials. *Carbohydrate Polymer*, *72*, 197–210.
Zablackis, E., Huang, J., Muller, B., Darvill, A. G., & Albersheim, P. (1995). Characterization of the cell-wall polysaccharides of *Arabidospsis thaliana* leaves. *Plant Physiology*, *107*, 1129–1138.